Journal of the Optical Society of Korea, Vol. 8, No. 4, December 2004, pp. 156-162

Spectroscopic Analysis of Gain Bandwidth in Raman Amplifier with Multiwavelength Pumping Scheme Using Actual Band Model

Georgii Felinskyi, Young-Geun Han*, and Sang Bae Lee

Photonics Research Center, Korea Institute of Science and Technology (KIST), 39-1 Hawolgok-dong, Seongbuk-gu, Seoul 136-791, KOREA

(Received January 9, 2004)

The spectroscopic model is proposed to analyze the gain bandwidth of a fiber Raman amplifier (FRA) with a multiple wavelength pumping scheme based on Raman gain theory. The oscillatory lineshape, which is the analytic function to analyze Raman gain spectra, allows us to estimate the gain bandwidth of the FRA. Based on the proposed theoretical modeling, we design and analyze the characteristics of the FRA using the combined multiwavelength pumping sources. We achieved the extended gain bandwidth of the FRA over 80 nm with the small gain ripple less than 0.5 dB. Threshold pumping power and effective noise figure for the FRA can be also analyzed by using the proposed model, which is also applicable for versatile fibers with other doping materials. The proposed analysis method can be useful for the design of the FRA with the multiwavelength pumping scheme.

OCIS codes : 060.2320, 170.5660

I. INTRODUCTION

Fiber Raman amplifiers (FRA) are being deployed in almost every new long-haul fiber-optic transmission system [1]. Despite the simple architecture of the FRA, many design factors like pump-to-pump power transfer, signal-to-signal power transfer, pump depletion (saturation), double Rayleigh scattering (multipath interference), and amplifier spontaneous noise should be considered to get broad gain bandwidth and small gain ripple [2]. In a previous report [2], eight evenly spaced pumps with equal pump power of 120 mW were used for the FRA with broad gain bandwidth. The gain variation, however, was more than 10 dB. In order to achieve broad gain bandwidth with small gain ripple, the power and wavelength of each pump laser diode (LD) should be carefully chosen.

It is not easy to directly obtain the gain profile of the FRA with the multiwavelength pumping scheme based on the coupled equations since the stimulated Raman scattering (SRS) process is so complicated. Numerical optimization methods for the optimization of the pumping power and wavelength such as simulated annealing algorithm [3], single-layer feedforward neural networks [4], and so on [5] have been investigated. The theoretical analysis of the Raman gain coefficient with one pumping wavelength in optical fiber and comprehensive analysis of its scaling with wavelength, modal overlap, and material composition are also reported [6]. In previous methods, however, pump power distributions that are undesirable in practice can be created due to an inadequate choice of frequency dependent factors like Raman gain coefficient and effective area when the pump wavelengths are automatically arranged corresponding to the wavelength of the Raman gain. All parameters of the FRA can be obtained by the propagation equations for signal and pump waves with a proper theoretical model in optical fibers.

In this paper, we will propose the spectroscopic model for the analysis of Raman gain spectrum based on the oscillator theory and its application to the design of the practical FRA with the multiwavelength pumping scheme. By introducing the oscillatory lineshape function of $S_R(v)$, we can analyze the amplification process of the FRA. The experimental configuration of the FRA with the broad gain bandwidth and small gain ripple is proposed and analyzed by the actual band model based on $S_R(v)$. The threshold pumping power and effective noise figure for the FRA can be also analyzed by the proposed model, which is also applicable for versatile fibers with other doping materials.

II. The SPECTROSCOPIC MODEL FOR FRA

Total amplified power over all signal bands of the FRA with one pumping source can be expressed by $P_{SIG}(z)=\int dv p_{SIG}(v,z)$, where $P_{SIG}(v,z)$ is the signal spectral power density and v is the Stokes frequency [7]. When pumping saturation is negligible, the signal spectral power density can be written as $p_{SIG}(v,z)=p_s(v,0)\exp\left[-\alpha z+\sigma(v)\left(1-e^{-\alpha z}\right)\right]$, where $p_s(v, z)$ is the Stokes power and α is the average fiber attenuation in the signal band and $1\sigma(v)=\sigma_0 S(v)$. The dimensionless function $S(v)$ is the normalized lineshape function so that its peak value is unity, and $\sigma_0=g_R P_0/(A_{eff}\alpha)$, where g_R is the peak Raman Stokes gain coefficient, P_0 is the input pump power, and A_{eff} is the effective area of the pump wave.

The pumping power saturation is not negligible in distributed FRA with multiple wavelengths pumping. The pumps depletion caused by the interaction between the pumps and the amplified signals is described by a well-known set of coupled equations [2-5,8]. Equations for the multiwavelength pumping scheme, which preserves the photon number and include the fiber loss $\alpha(v,T)$ and Rayleigh backscattering $\gamma_b(v)$, can be expressed as [5]

$$\begin{aligned}\pm\frac{dP_i^{\pm}}{dz}=&-\alpha(v_i,T)P_i^{\pm}+\gamma_b(v_i)P_i^{\mp}+P_i^{\pm}\sum_j^{v_j>v_i}\frac{g_R(v_j,v_i)}{A_{eff}(v_j,v_i)}\left(P_j^{+}+P_j^{-}\right)\Delta v\\&+2\sum_j^{v_j>v_i}\left(P_j^{+}+P_j^{-}\right)hv_i\Delta v\frac{g_R(v_j,v_i)}{A_{eff}(v_j,v_i)}\cdot\left[n_B(v_j-v_i)+1\right]\\&-P_i^{\pm}\sum_j^{v_i<v_i}\frac{V_j}{V_i}\frac{v_i}{v_j}\frac{g_R(v_i,v_j)}{A_{eff}(v_i,v_j)}\left(P_j^{+}+P_j^{-}\right)\Delta v\\&+2\sum_j^{v_i<v_i}\left(P_j^{+}+P_j^{-}\right)hv_i\Delta v\frac{v_i}{v_j}\frac{V_j}{V_i}\frac{g_R(v_i,v_j)}{A_{eff}(v_i,v_j)}\cdot n_B(v_i-v_j)\end{aligned},\quad(1)$$

where the subscript i represents the ith wavelength with frequency v_i and V_i, P_i are the group velocity and optical powers, respectively. $A_{eff}(v)$ is fiber effective area and $g_R(v_i,v_j)$ is the Raman gain coefficient at signal frequency (v_j) and pumping frequency (v_i). In eq. (1), the multiple channels with the optical bandwidth of Δv are included in the codirection (superscript "+") and counterdirection ("-"). $n_B(v)=[\exp(hv/kT)-1]^{-1}$ is the phonons' Bose-Einstein distribution, where h is Planck's constant, k is the Boltzmann constant, T is the temperature. n_B+1 describes the Stokes component of the amplified spontaneous emission (ASE) generation, and n_B describes the anti-Stokes ASE generation, which are the results of photon number conservation. In general, the frequency dependence of the Raman gain coefficient $g_R(v)\sim S(v)$ at each pumping wavelength is determined by the lineshape function of $S(v)$ in accordance with the stimulated Raman scattering process. The Raman gain coefficient is a fundamental parameter for the Raman amplification.

When the frequency dependence of the Raman gain $g_R(v)$ is modeled as a frequency independent constant or simple single peak, for example as a triangle, the numerical methods may give unsatisfactory results because the solutions of the coupled equations (1) are very sensitive to absolute values of equation coefficients. If the determination of $g_R(v_i,v_j)$ in eq. (1) is inaccurate, the numerical methods can not be capable of fully handling the FRA optimization problem. It is necessary to take into account the material parameters of fibers in the FRA.

SRS process has the frequency shifted Stokes within the line of spontaneous scattering by vibration modes of fiber material. According to the semi-classical derivation [6], SRS can be described in terms of classical optical fields and the molecular system can be treated as a forced harmonic oscillator. This model reveals the connection between the differential polarizability ($\partial\alpha_{ij}/\partial q_n$) of a molecular lattice and complex value of its nonlinear susceptibility $\chi^{(3)}$, which is traditionally used in nonlinear optics and can be written as

$$\chi_{ijkl}^{(3)}=\frac{N}{12m\varepsilon_0 V}\frac{1}{\omega_v^2-\omega^2+2i\omega\Gamma}\cdot\sum_n\frac{\partial\alpha_{ij}}{\partial q_n}\left(\frac{\partial\alpha_{kl}}{\partial q_n}\right)^{*},\quad(2)$$

where ω_v is the undamped resonance phonon frequency, ω is the angular frequency of a phonon, Γ is the phonon damping constant, q_k is the coordinate that describes the local displacement that results from the time-dependent electric field, m is the mass associated with the vibration, N is the number of oscillators in the interaction volume V, ε_0 is the vacuum permittivity. Since an optical fiber is made of a silica glass, which is an amorphous material, the fourth-rank tensor $\chi^{(3)}$ is isotropic. Thus, $\chi^{(3)}$ has only 21 nonzero elements and their indexes are identical to $\chi_{iiii}^{(3)}$ or occur in pairs $\chi_{ijji}^{(3)}$, $\chi_{ijij}^{(3)}$, and $\chi_{iijj}^{(3)}$. Therefore, the Raman gain coefficient in the Stokes frequency $\omega_s=\omega_p-\omega_v$ can be written as [6]

$$g_R=-\frac{3\omega_s}{\varepsilon_0 c^2 n_p n_s}\frac{\mathrm{Im}\left[\chi_{iiii}^{(3)}+\chi_{ijji}^{(3)}\right]}{2A_{eff}^{ps}}.\quad(3)$$

Assuming that the third-order susceptibilities are frequency-independent, it is noticeable that the gain coefficient g_R linearly depends on the frequency of the Stokes-shifted wave, and its frequency dependence can be described by the imaginary part of nonlinear susceptibility $\chi^{(3)}$ like the resonant denominator of phonon harmonic oscillator.

III. ACTUAL BAND MODEL

The frequency distribution of Raman cross section is described by two types of lineshape $S(v)$ functions in spectroscopy. The Lorentzian lineshape $S_L(v)$ can be

written as [7,9]

$$S_L(v)=\frac{(w/2)^2}{(v-v_0)^2+(w/2)^2}, \quad (4)$$

where v_0 is the center frequency and w is the full width at half maximum (FWHM). This function is widely used for many spectroscopic models, particularly Raman scattering. From eq. (2) and (3), the frequency dependence of Raman gain $S(v)$ can be written as

$$S(v)=-\mathrm{Im}\left[\frac{1}{v_0^2-v^2+i\nu\gamma}\right]=\frac{\nu\gamma}{\left(v_0^2-v^2\right)^2+v^2\gamma^2}, \quad (5)$$

where the $v's$ are wave numbers (v_0, $\omega_v/2\pi c$, $v=\omega/2\pi c$, and $\gamma=\Gamma/\pi c$) and γ is approximately the FWHM of $S(v)$. The normalized function of $S_R(v)$ is the lineshape function, which is dimensionless, and can be written as

$$S_R(v)=\gamma v_0 S(v)$$
$$S_R(v_0)=1$$

Since the Stokes shifted line profile of Raman gain in SRS process repeats the line form of phonon vibrations in fiber material, the lineshape functions of $S_L(v)$ and $S_R(v)$ can be useful for modeling of Raman amplification. The Lorentzian lineshape of $S_L(v)$ is very closed to the normalized curve $S_R(v)$ for the phonon harmonic oscillator, especially, when $v_0>>w,\gamma$, as shown in Fig. 1. A small shift at line center frequency of $S_R(v)$ in comparison with $S_L(v)$ deals with influence of the pumping shift on the phonon harmonic oscillator. The amount of the shift increases with γ because the maximum value of the Lorentzian function is equal to unity ($S_L(v_0)=1$) and independent of γ at v_0. The large difference is visible in the low frequency as shown in Fig. 2. In contrast with the oscillatory function ($S_R(0)=0$), the Lorentzian function is not zero at $v=0$. The small difference between two curves of $S_L(v)$ and $S_R(v)$ takes place in the long wavelength region. The integral intensity of both line shapes, however, remains almost the same at $v_0>>w,\gamma$. We use the oscillatory function of $S_R(v)$ in our modeling in accordance with the conventional Raman gain theory. Fig. 3 (a) and (b) show the measured results of Stokes Raman line with 20 mol. % GeO_2 [10] and the theoretical results based on the proposed lineshape function of $S_R(v)$ (dotted line in Fig. 3 (b)), respectively. When the undamped resonant phonon frequency (v_0) and photon damping constant (γ) are 435 cm^{-1} and 130 cm^{-1}, respectively, the phonon harmonic oscillator function of $S_R(v)$ becomes the best fitting curve to experimental data of the Raman gain in highly Ge-doped fibers as seen in Fig. 3 (b).

To estimate the fitting accuracy we used the square-law deviation $\sigma^2=[S_R(v)-S_{exp}(v)]^2/S^2_{exp}(v_0)$ for the variation of the oscillator lineshape function of $S_R(v)$ obtained from the experimental result of the gain profile $S_{exp}(v)$, which shown in Fig. 3 (b). It should be noted that $\sigma^2<$ 1% for all wave numbers, which ranged from 100 cm^{-1} up to 600 cm^{-1}, and its average value was $\sigma^2=0.2\%$. In addition, good conformity between theoretical and experimental results could be obtained and the difference of the integrated intensity in the gain profile was less than on 0.8% in the specified amplification band.

We applied the proposed modeling method to the analysis of the amplification process in the FRA. For each doping material with the one dominant vibration mode, it is necessary to get two parameters like the central vibration frequency and its dumping constant in the lineshape function of $S_R(v)$. In many cases, it is expedient to use one actual band for the effective

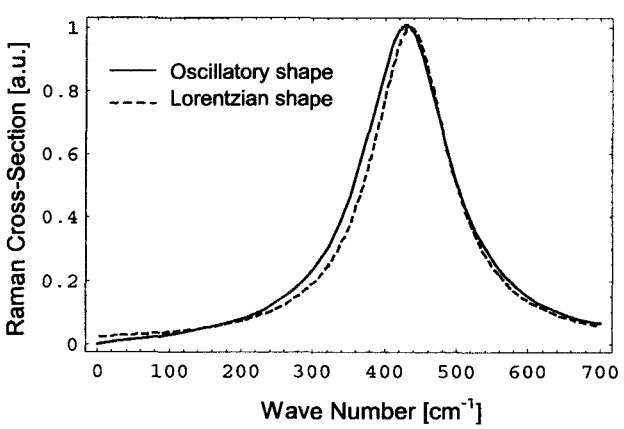

FIG. 1. Lineshape functions: Lorentzian $S_L(v)$ (dotted line) and oscillatory shape $S_R(v)$ (solid line) under v_0=435 cm^{-1}, $w/2=\gamma$ =130 cm^{-1}.

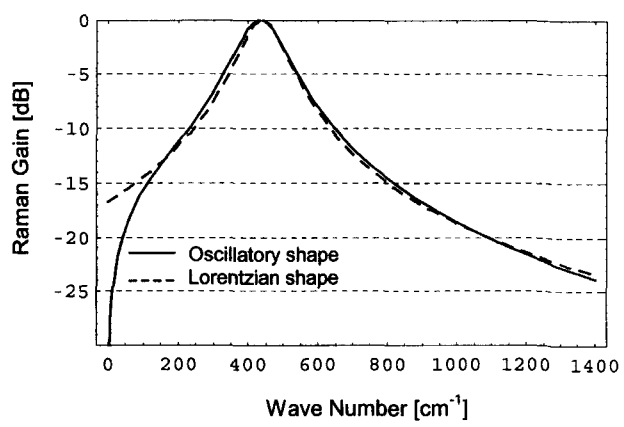

FIG. 2. Lineshape functions $S_L(v)$ (dotted line) and $S_R(v)$ (solid line) are shown in logarithmic scale. Parameters are the same as in Fig. 1.

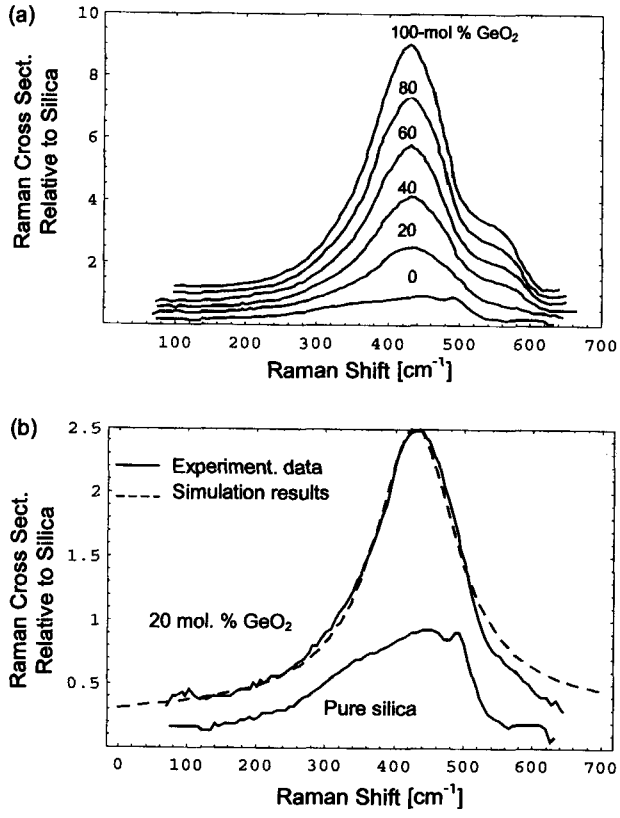

FIG. 3. (a) Experimental measurements of zero Kelvin Raman cross-section relative to silica in germanosilicate glass [9] (solid lines) and (b) approximation of the Stokes Raman line in 20 mol. % GeO_2 by $S_R(v)$ function (dotted line).

account and to display several spectral bands to analyze the complex spectra with many overlapped lines. The real multiple spectra can be represented by one spectral component, which gives the maximal spectrum profile and the approximation of the integrated intensity. The resulting component with proper lineshape $S_R(v)$ is called the actual band for a real spectrum. The concept of the actual band has been frequently used in spectroscopy. It is also useful for the analysis and synthesis of the Raman spectra with the multiwavelength pumping scheme. The actual band approximation of the Raman gain provides a good fitting curve in Ge-doped fibers as seen Fig. 3, but the conformity is not good for the case of pure silica fibers.

Based on the actual band model in the Raman gain, we obtain the amplified stimulated emission (ASE) spectra to compare with the experimental results of the effective noise figure with respect to wavelength [11]. Fig. 4 shows the theoretical results of ASE spectra (solid line) for 6 wavelengths pumped Raman amplifier in both C- and L-bands. We compared our simulation results with experimental data for the effective noise figure [11] (points with dashed lines in Fig. 4). Six

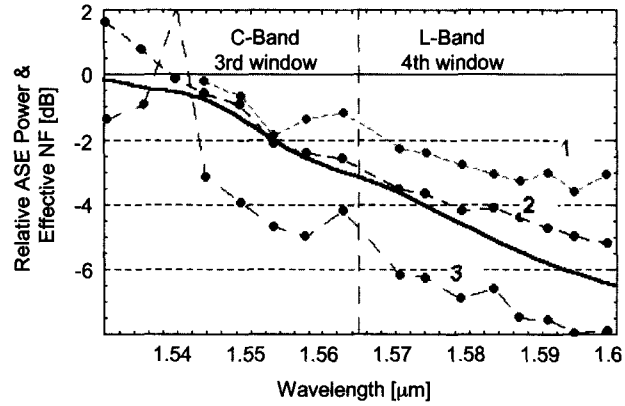

FIG. 4. Simulated relative ASE spectra (solid line) and measured effective noise figure for 6 wavelengths pumped Raman amplifier in C + L band. 1 – 60 km; 2 – 100 km; 3 – 140 km (Exp. data from [11]).

wavelengths (1428, 1445, 1466, 1480, 1494 and 1508 nm with pumping powers of 338, 215, 83, 30, 19, and 39 mW, respectively) were used in experiment [11]. These wavelengths were chosen to uniformly distribute the pumps in the optical frequency.

Modeling conditions are as followed. The ASE spectral density at the FRA output should have the same form as the Raman gain profile at the uniform distribution of optical noise. We have modeled the gain profile band based on the pumping wavelengths and pumping powers data as given in Ref. [11]. The ASE results in the frequency dependence of the noise figure over the FRA bandwidth. The shape of the noise figure is proportional to the ASE distribution at the FRA output in experimental conditions of Ref. [11], when the gain ripple is minimal. The slope of the ASE distribution was ~7 dB in both C- and L-bands. This value was good agreement with the noise figure slopes (approximately 7 dB) in all fiber lengths of 60 km, 100 km, and 140 km as seen in Fig. 4. The noise figure in the FRA is mainly formed at near to the pump sources because the pumping power is maximal. General pumping losses including the pump depletion during the propagation through the fiber reduces the pumping power and it becomes insufficient for the ASE generation. Therefore, the average slopes of the noise figure become constant regardless of the various fiber lengths and finally they are the same as the ASE distribution in Fig. 4. Therefore, the actual band model allows us to get the information about the nature of the formation mechanism of the noise parameters in the practical FRA as well as the bandwidth of the FRA.

To verify that the proposed spectroscopic model is applicable for the analysis of the Raman gain spectra with any complexity, it is necessary to use the multiple vibrational mode model with the appropriate set of approximating functions for each participating oscillation

in the SRS process.

IV. THEORETICAL RESULTS

The spectroscopic model allows us to estimate the gain bandwidth of FRA with the multiply pumping sources. Based on the proposed model, it is easy to obtain the gain bandwidth of FRA without solving the coupled waves equations. We applied the proposed spectroscopic model to analyze the FRA with four pump sources (1426, 1436, 1456, and 1466 nm) with the maximum pump power of 300 mW. In Fig. 5 (a), the bandwidth of the FRA at 1 dB level was about 50 nm in the range from 1520 nm to 1570 nm and its gain ripple was about 0.5 dB. After measuring the FRA for 980 SMF and ordinary SMF, which are the same length of 340 m, we compared the theoretical and experimental results as seen in Fig. 5 (b). The theoretical results based on the proposed model have the good conformity with experimental ones as seen in Fig. 5 (b). The gain ripple of the FRA in the wavelength range from 1528 nm to 1562 nm was about 1 dB.

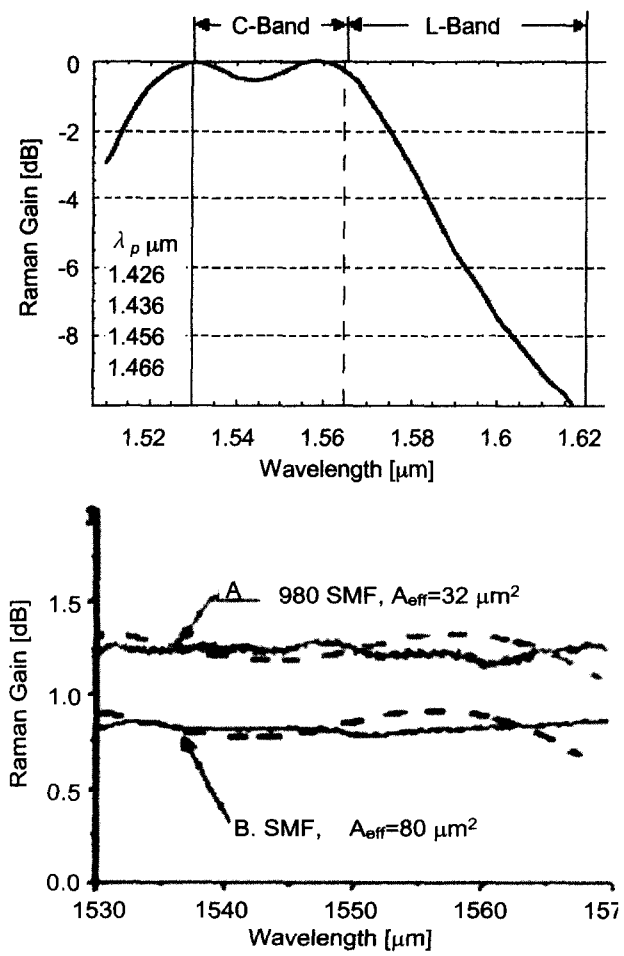

FIG. 5. (a) The calculated gain bandwidth of the FRA with 4 LDs pumping based on actual band model and (b) theoretical (dashed Line) and experimental (solid lines) results of the Raman gain in C-band for 980SMF fiber (A_{eff}=32 μm^2, length=340 m : A) and SMF fiber (A_{eff}=80 μm^2, length=340 m : B).

The gain bandwidth of the FRA can be extended to the L-band if two pumping sources at 1486 nm and 1510 nm are added. Fig. 6 shows the experimental schematic of the FRA with six pumping sources for the extension of its gain bandwidth to L-band. It is composed of 4 pumping LDs (λ_p=1426, 1436, 1456, and 1466 nm) and two grating cavities (1486 and 1510 nm). The pumping power at long wavelength can be enhanced by the interaction between short and long wavelength pumping sources in a distributed Raman amplifier. To improve the gain flattening of the FRA with the multiwavelength pumping scheme, 10% of pumping power at short wavelength should be used for amplification and the rest will be utilized for the generation of other pumping sources at long wavelength based on fiber grating cavity. After analyzing the Raman gain based on the proposed theoretical model, the pumping power was adjusted to optimize the gain flatness of the FRA. The ratio of the effective pumping powers was 0.8 : 1.0 : 0.75 : 0.7 : 1.1 : 1.5. Compared with the experimental result in Fig. 5 based on 4 LDs pumping scheme, we could obtain the extended bandwidth of the FRA ranged from C-band to L-band with the small gain ripple. Fig. 7 shows the theoretical results of the FRA with the wide bandwidth over 80 nm and the low gain ripple less than 0.5 dB.

The threshold power of pumping source can be achieved if the input pumps power for the pure amplification of the spontaneous Stokes emission becomes higher than fiber loss, α_s. the lasing threshold pump power, $P_p(w)$, can be found when the pump wave interacts with the spontaneous Stokes wave, which can generate the stimulated power $P_s(\omega)$ [8]. The propagating Stokes wave in the z-direction along the fiber increases under the condition of $P_p(\omega) \geq \alpha_s A_{eff}/g_R(\omega)$ $(dP_s(\omega)/dz>0)$. Since the proposed spectroscopic model can give the function of $g_R(\omega)$, we can get the thre-

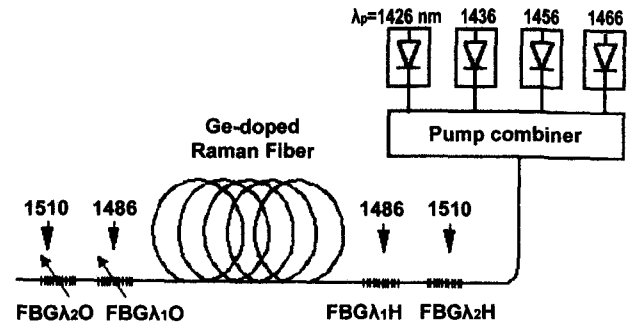

FIG. 6. Experimental setup of 6 pumping sources for the FRA with the extended bandwidth to L-band.

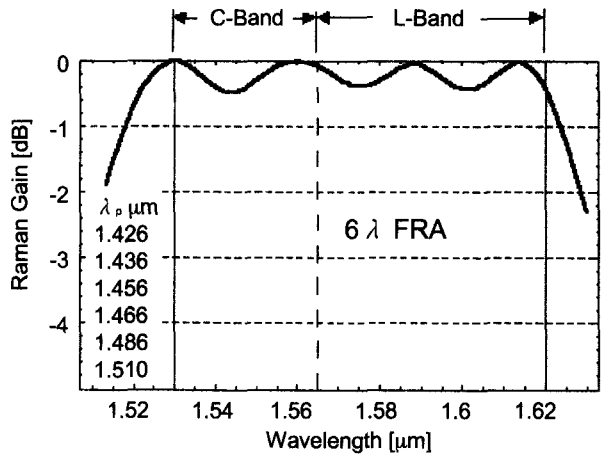

FIG. 7. Raman gain of the FRA with the broad bandwidth over 80 nm and the small gain ripple <0.5 dB. The ratio of effective pumping powers is 0.8 : 1.0 : 0.75 : 0.7 : 1.1 : 1.5.

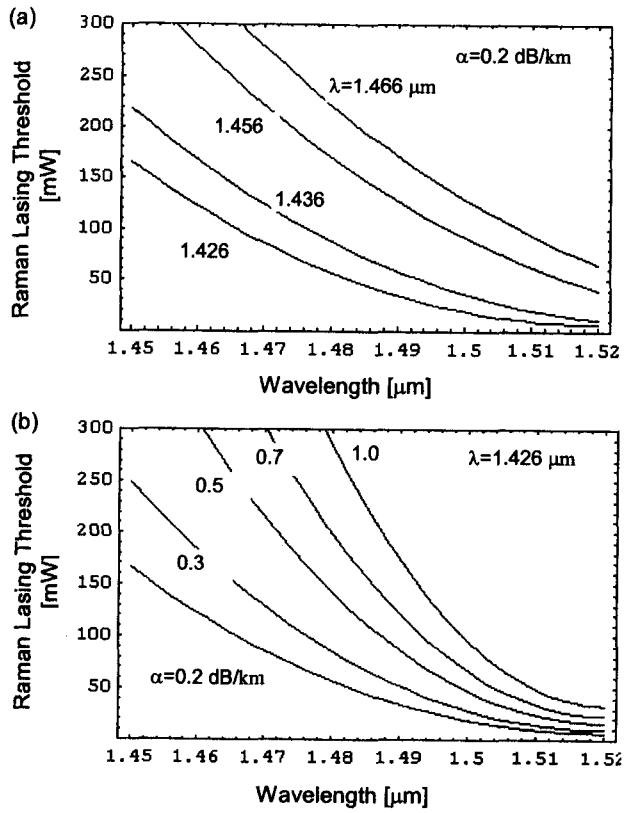

FIG. 8. (a) Threshold pumping power for Raman lasing with respect to the different pumping wavelength and (b) the variation of the threshold pumping power at 1.426 nm according to different optical loss in Ge-doped fibers for g_{max} (Raman fiber GeO_2) = 6.1 $(W \cdot km)^{-1}$ [12].

shold power of the pumping source to get a gain. Fig. 8 (a) shows the threshold power of each pump source when the fiber loss was 0.2 dB/km and Fig. 8 (b) shows the threshold power at 1426 nm with the variation of the fiber loss. The detailed parameters of each pumping source with grating cavities are shown in Table 1.

TABLE 1. Threshold powers for Raman lasing on λ_l corresponding to pumping sources on λ_p.

Pumping λ_p, μm	Threshold power in mW for Raman lasing at λ_l, μm	
	1.486	1.510
1.426	42.6	9.7
1.436	69.6	20.3
1.456	144.0	62.7
1.466	190.9	93.9

V. CONCLUSION

In summary, the spectroscopic model was investigated for the design of the FRA with the multiwavelength pumping sources based on the Raman gain theory. The oscillatory lineshape functions of $S_R(v)$ can simply describe the wavelength dependence of Raman gain in optical fibers and is very useful for the estimation of the gain bandwidth, Raman lasing, noise performance, and amplification processes in Raman amplifiers. The concept of an actual band based on the lineshape function of $S_R(v)$ is useful for the design of the FRA with the multiwavelength pumping scheme. Using the proposed actual band model, we obtained the parameters of FBG and lasing thresholds that were good agreement with experimental parameters for the FRA in Ge-doped fibers. In addition, the proposed theoretical model allows us to get the information about the mechanism of the noise parameters formation in the practical FRA. The proposed spectroscopic model can be further extended for the analysis of the complex SRS spectra with other doping materials.

*Corresponding author : yyghan@kist.re.kr

REFERENCES

[1] M. N. Islam, "Raman Amplifiers for Telecommunications," *IEEE J. Sel. Top. Quantum. Electron.*, vol. 8, no. 3, pp. 548-559, 2002.

[2] H. Kidorf, K. Rottwitt, M. Nissov, M. Ma, and E. Rabarijaona, "Pump interactions in 100 nm bandwidth Raman amplifier," *IEEE Photon. Technol. Lett.*, vol. 11, no. 5, pp. 530-532, 1999.

[3] M. Yan, J. Chen, W. Jiang, J. Li, J. Chen, and X. Li, "Automatic Design Scheme for Optical-Fiber Raman Amplifiers Backward-Pumped With Multiple Laser Diode Pumps," *IEEE Photon. Technol. Lett.*, vol. 13, no. 9, pp. 948-950, 2001.

[4] P. Xiao, Q. Zeng, J. Huang, and J. Liu, "A New

Optimal Algorithm for Multipump Sources of Distributed Fiber Raman Amplifier," *IEEE Photon. Technol. Lett.*, vol. 15, no. 2, pp. 206-208, 2003.

[5] I. Mandelbaum and M. Bolshtyansky, "Raman Amplifier Model in Single-Model Optical Fiber," *IEEE Photon. Technol. Lett.*, vol. 15, no. 12, pp. 1704-1706, 2003.

[6] K. Rottwitt, J. Bromage, A. J. Stentz, L. Leng, M. E. Lines, and H. Smith, "Scaling of the Raman Gain Coefficient: Applications to Germanosilicate Fibers," *J. Lightwave Techn.*, vol. 21, no. 7, pp. 1652-1662, 2003.

[7] M. L. Dakss and P. Melman, "Amplified Spontaneous Raman Scattering and Gain in Fiber Raman Amplifiers," *J. Lightwave Technol.*, vol. LT-3, no. 4, pp. 806-813, 1985.

[8] G. P. Agrawal, *Nonlinear Fiber Optics*, second ed. San Diego, CA: Academic. 1995.

[9] R. Loudon, *The Quantum Theory of Light*, second ed. Clarendon Press, Oxford, 1983.

[10] S. T. Davey, D. L.Williams, and B. J. Ainslie, "Optical gain spectrum of GeO_2 -SiO_2 Raman fiber amplifiers," *Proc. Inst. Elect. Eng.*, vol. 136, no. 6, pp. 301-306, 1989.

[11] M.D. Mermelstein, C. Horn, S. Radic, and C. Headley, "Six-wavelength Raman fibre laser for C- and L-band Raman amplification and dynamic gain flattening," *Electronics Letters*, vol. 38, no. 13, pp. 636-638, 2002.

[12] J. Bromage, K. Rottwitt, and M. E. Lines, "A method to predict the Raman gain spectra of germanosilicate fibers with arbitrary index profiles," *IEEE Photon. Technol. Lett.*, vol. 14, no. 1, pp. 24-26, 2002.